Received: 11 August 2022 | Revised: 2 November 2022 | Accepted: 5 November 2022

DOI: 10.1002/psp4.12895

ARTICLE

Interspecies and in vitro-in vivo scaling for quantitative modeling of whole-body drug pharmacokinetics in patients: Application to the anticancer drug oxaliplatin

Simona Catozzi[1] | **Roger Hill**[2] | **Xiao-Mei Li**[3] | **Sandrine Dulong**[1,3] | **Elodie Collard**[4] | **Annabelle Ballesta**[1]

[1]Institut Curie, Inserm U900, MINES ParisTech, CBIO - Centre for Computational Biology, PSL Research University, Saint-Cloud, France

[2]EPSRC and MRC Centre for Doctoral Training in Mathematics for Real-World Systems, University of Warwick, Coventry, UK

[3]UPR "Chronotherapy, Cancers and Transplantation," Faculty of Medicine, Université Paris-Saclay, Villejuif, France

[4]CEA, CNRS, NIMBE, Université Paris-Saclay, Gif-sur-Yvette, France

Correspondence
Simona Catozzi, Institut Curie, 35 Rue Dailly, 92210 Saint-Cloud, France.
Email: simona.catozzi@curie.fr

Abstract

Quantitative systems pharmacology holds the promises of integrating results from laboratory animals or in vitro human systems into the design of human pharmacokinetic/pharmacodynamic (PK/PD) models allowing for precision and personalized medicine. However, reliable and general in vitro-to-in vivo extrapolation and interspecies scaling methods are still lacking. Here, we developed a translational strategy for the anticancer drug oxaliplatin. Using ex vivo PK data in the whole blood of the mouse, rat, and human, a model representing the amount of platinum (Pt) in the plasma and in the red blood cells was designed and could faithfully fit each dataset independently. A "purely physiologically-based (PB)" scaling approach solely based on preclinical data failed to reproduce human observations, which were then included in the calibration. Investigating approaches in which one parameter was set as species-specific, whereas the others were computed by PB scaling laws, we concluded that allowing the Pt binding rate to plasma proteins to be species-specific permitted to closely fit all data, and guaranteed parameter identifiability. Such a strategy presenting the drawback of including all clinical datasets, we further identified a minimal subset of human data ensuring accurate model calibration. Next, a "whole body" model of oxaliplatin human PK was inferred from the ex vivo study. Its three remaining parameters were estimated, using one third of the available patient data. Remarkably, the model achieved a good fit to the training dataset and successfully reproduced the unseen observations. Such validation endorsed the legitimacy of our scaling methodology calling for its testing with other drugs.

Study Highlights

WHAT IS THE CURRENT KNOWLEDGE ON THE TOPIC?

Drug development is often hindered by difficulties in generating patient data. Quantitative systems pharmacology (QSP) offers to combine preclinical and clinical results for time- and cost-effective clinical trial design.

WHAT QUESTION DID THIS STUDY ADDRESS?

A current bottleneck of QSP is the lack of reliable interspecies/-scale methodologies accurately integrating preclinical and clinical results into human pharmacokinetic/pharmacodynamic (PK/PD) models. Such challenge is complicated by in vitro-in vivo differences in drug PKs, and by species-specific expression of the proteins interacting with a given drug.

WHAT DOES THIS STUDY ADD TO OUR KNOWLEDGE?

Focusing on oxaliplatin, we developed: (i) an interspecies scaling methodology to integrate ex vivo PK data from the mouse and rat to inform the human model, and (ii) a multiscale approach to design a whole-body human PK model for clinically relevant predictive purposes.

HOW MIGHT THIS CHANGE DRUG DISCOVERY, DEVELOPMENT, AND/OR THERAPEUTICS?

The proposed approach allows for reliable design of human PK models that constitute critical tools for personalizing drug dose and timing toward high patient benefit.

INTRODUCTION

Physiologically-based pharmacokinetic (PBPK) modeling is currently a widely used strategy to explore and guide the design of experiments, from the preclinical to the clinical phases.[1,2] This approach combines in vitro and in vivo data with in silico studies, and is suitably used for drug discovery and development.[3,4] In particular, its usefulness has been acknowledged through the regulatory support from both the US Food and Drug Administration[5] and the European Medicines Agency.[6] Patient eligibility to a certain treatment, prediction of the effect of varying drug regimens and doses, or simulation of physiological and biochemical variability (e.g., due to species, pediatric age, pregnancy, obesity, disease state, etc.), are some of the applications of such multiscale methodologies.

The integration of in vitro, preclinical, and clinical data is at the core of quantitative systems pharmacology (QSP), and is especially useful when assessment is unlikely to be performed directly on patients.[3] QSP models represent the different organs/tissues as a series of compartments connected by flow rates, and describe prior knowledge in mechanistic terms (i.e., relying on the physiology and the molecular events of drug action). One of the key challenges resides in model calibration, which requires data availability that is often sparse in patients. To address this issue, QSP offers to use preclinical datasets to calibrate human models through accurate interspecies scaling and/or in vitro-to-in vivo extrapolation (IVIVE).[7]

IVIVE methods are promising tools as they aim to develop human PBPK models using in vitro or ex vivo data, with the purpose to replace, reduce, and refine animal use, and improve time- and cost-effectiveness, for risk and safety assessment of medical products.[8] However, such methodology is challenging to develop as, for instance, bioavailability of drugs may depend on multiple factors related to the specific in vitro system such that nonspecific migration to plastics, binding to media constituents, evaporation, degradation, or metabolization.[9] Thus, existing strategies for IVIVE scaling all tend to be specific to the in vitro system considered, which justify why their use in the regulatory domain lacks acceptance so far.[8] In parallel, interspecies scaling strategies have been developed in an attempt to predict human pharmacokinetics (PKs) from experimental animal studies (e.g., mice, rats, monkeys, etc.). The most widely developed ones are allometry-based (i.e., size-dependent) approaches which assume that human parameters may be inferred from animal parameters adjusted by a correction factor, based on body weight or body surface (i.e., $P = a\mathrm{BW}^m$, where P is a physiological property, a an empirical coefficient, BW the body weight, and m the allometric exponent).[10–18] However, predicting human PK leveraging on preclinical data that come from other species requires a quantitative translation of the drug fate and action that the allometric scaling laws generally are unable to reflect. Hence, interspecies differences in drug metabolism and PKs usually preclude realistic estimations of human PKs.[19] Despite some recent examples of successful translational interspecies scaling based on PBPK models,[20–22] the lessons learned from both IVIVE and allometric scaling methods report the complexities of developing multiscale approaches for trustworthy predictions, and point out the relevance of accounting for species-specific physiological and molecular parameters. Thereby, in order to efficiently guide the design of

clinical trials, the conception of a general framework for translational scaling is still an unmet need in the field of QSP.[23]

The goal of this study was to derive a general scaling methodology to integrate preclinical data into the design of clinical PBPK models for any compound, including those under development for which little human data are available. We designed such an approach for one of the most commonly used anticancer drug against digestive cancers, oxaliplatin, for which extensive preclinical and clinical were available or generated to allow for full validation.[24] We present an IVIVE and rodent-to-human scaling approach with a rational selection of parameter estimation strategies, based on model error, parameter estimate confidence intervals, and parameter identifiability. Oxaliplatin is responsible for severe side effects, and large interpatient variability in toxicities and efficacy has been described.[25] Patient's sex plays a critical part, in fact, oxaliplatin hematological toxicities were almost twice as large in women as compared with men.[26] Oxaliplatin circadian timing of administration also led to differences in patients' with colorectal cancer survival in a sex-dependent manner.[27] Hence, mechanistic PK/pharmacodynamic (PD) models tailored to individual patient's physiology would allow to personalize drug dose and timing, in order to maximize the patient's benefit.

Oxaliplatin contains molecules of platinum (Pt), which can irreversibly bind to plasma proteins (primarily to albumin and gamma-globulins) and red blood cells (RBCs), becoming partitioned in the blood under three forms: total Pt, ultrafilterable (free) Pt, and RBC Pt.[28–30] In humans, more than 90% of the drug is found in a bound state, 6 h after administration,[31] and the binding rate is known to vary across species, likely as a result of the different relative concentrations of the amount of plasma proteins in the blood.[32] Importantly, this Pt-protein interaction has been shown to affect both the PK properties and the antitumor efficacy of the treatment.[33]

Here, we first created a model of oxaliplatin ex vivo PK in the whole blood (comprising plasma and RBC compartments) that was calibrated on ex vivo data coming from three different species (the mouse, rat, and human). We developed a combined physiologically based strategy for interspecies scaling, and parameter estimation and identifiability were extensively investigated. Then, building on these premises, we established a comprehensive whole-body model of oxaliplatin PKs, incorporating, to the former whole-blood model, two additional compartments for liver and other non-eliminating organs. It was thus calibrated using mainly preclinical data, and a minimal subset of human data, and this enabled accurate reproduction of unseen observations. This validation therefore endorsed the legitimacy of our ex vivo-to-in vivo scaling method.

METHODS

Ex vivo time-dependent Pt measurements in mouse whole blood

All procedures were performed in accordance with the French guidelines for animal care and experimentation (Directive 2010/63 and Decree 2013-118 associated with 5 implementing laws). The project was approved by the French Ministry of Research and Innovation (approval number APAFIS 13311-2018020113435820). Sixteen 8-week-old C57BL/6 male mice were kept in 12 h light/12 h dark cycles (LD 12:12) for 1 week. The blood of healthy animals was collected using cardiac puncture after anesthesia at ZT3. The whole blood of four to five mice was pooled in a total of three heparinized tubes, maintained at 5% CO_2 at 37°C and stirred during the whole experiment. Oxaliplatin treatments with 20 µg/ml were applied to the tubes at time $t = 0$, and 0.5 ml aliquots were sampled at $t = 0$, 0.5, 1, 2, 4, and 6 h. Samples were immediately centrifuged at 2000*g* for 10 min at 4°C to separate the plasma and the RBCs. Then, 150 µl of plasma were mixed to 150 µl of phosphate-buffered saline (PBS) and filtered through Amicon ultra-0.5 centrifugal filter devices (Mr cutoff = 10 kD) and centrifuged at 2000*g* for 20 min to obtain ultrafiltrate samples. The RBCs were washed three times with cold PBS buffer and re-suspended in 250 µl of cold PBS. About 150 µl of plasma, 250 µl of RBCs and plasma-ultrafiltrate were stored at −80°C until Pt determination.

Acidic lysis using one volume of nitric acid 70% during 30 min at 50°C were done to separate Pt. Samples were then diluted in chloridric acid 2% and applied for Pt measurement using mass spectrometry. Pt determination was performed by quadrupole ICPMS (iCapQ – Thermo Element). The instrument was equipped with a concentric nebulizer (conikal 1 ml/min) and a cyclonic nebulization chamber. Pt was measured on masses of 194, 195, and 196 with six runs by analysis. Standard Pt solutions were prepared by weight dilution in HCl 2% (prepared from suboiling distilled 37% chloridric acid) of standard 10,000 mg/L Pt (Spex-CertiPrep). The quality of the calibration was controlled every 10 samples.

Ex vivo time-dependent Pt measurements in rat whole blood

The rat ex vivo data come from males of 6–8 weeks and ~225 g of body mass.[34] The animals were synchronized by LD 12:12 at a temperature of 22°C for at least 1 week prior to the experiment. They were euthanized and 4.75 ml of heparinized blood (250 units heparin/ml) were mixed

with 0.25 ml of oxaliplatin stock solution (400 µg/ml or 1 mM) to obtain an initial oxaliplatin concentration of 50 µM. The mixture was then incubated in 5% CO_2 at 37°C for up to 24 h. Aliquots of 0.5 ml were taken subsequently at 0, 0.5, 1, 2, 4, 7, 9, and 12 h, after initial mixing. The samples were then analyzed for Pt recovery as bound or ultrafiltrate Pt in the plasma and the RBCs.

Ex vivo time-dependent Pt measurements in human whole blood and oxaliplatin PK in patients with cancer

Oxaliplatin was mixed with human blood and incubated at 37°C.[35] Aliquots of 1 ml were taken at 0, 1, 2, 3, 4, 5, and 6 h post mixing, and analyzed for Pt content in the plasma (ultrafiltrate and total Pt) and the RBCs. Three separate experiments were undertaken for oxaliplatin concentrations of 5, 10, and 20 µg/ml. The results were collated because there was no significant effect of the initial drug concentration on the percentage of total Pt recovered in each compartment.

The in vivo human data came from patients (7 men and 6 women) with advanced-stage solid tumors and normal renal function receiving oxaliplatin (130 mg/m^2) administered over a 2 h infusion.[36] Blood samples were taken before, during, and after the treatment, and were assessed for Pt concentration in the total plasma, the plasma ultrafiltrate, and the RBCs. Individual data points were used to compute means and SDs as follows. Data points were aggregated by bins of duration 0.5 h over the first 4 h when the kinetics was stiff, and of 4 h subsequently, ensuring to have at least two points per time interval.

Mathematical modeling and parameter estimation

The physiologically-based (PB) model of Pt ex vivo PKs in the whole blood was based on ordinary differential equations, solved using the ode45 solver from Matlab (R2021b, MathWorks). Model parameters were estimated using a least squares approach.[37] The model goodness-of-fit was assessed by:

$$\mathcal{L}^2(\theta) = \frac{1}{N}\sum_{i=1}^{N}\left(\frac{y_i - f\left(\theta, t_i\right)}{\sigma_i}\right)^2$$

where y_i and σ_i are respectively mean and SD of the measured value at time t_i, and $f\left(\theta, t_i\right)$ the value predicted by the model, at time t_i, with parameters $\theta \in \left(R^+\right)^N$. The optimal parameters $\hat{\theta}$ were defined by:

$$\hat{\theta} = \arg\min_{\theta}\left(\mathcal{L}^2(\theta)\right).$$

The numerical minimization task was performed using the Covariance Matrix Adaptation Evolution Strategy (CMAES) programmed in Matlab, which is successful at handling complex cost function landscapes involving a large number of parameters and possible local minima.[38] The search interval for the parameters was set to [0.01, 10]. To avoid possible local minima, we started with five different initial guesses for each parameter, uniformly chosen over the search interval.

The model-to-data error $\mathcal{E}^2$ was classically defined as:

$$\mathcal{E}^2 = \mathcal{L}^2\left(\hat{\theta}, t_i\right).$$

The combined error for multispecies simultaneous fit was defined as the sum of the model error for each species.

To compare the goodness-of-fit of the model in different scenarios, we defined the metric $\mathcal{G}$ as the ratio between the error obtained for one species independent fit and the error derived from the current multispecies fit:

$$\mathcal{G} = \frac{\mathcal{E}^2_{\text{indep fit}}}{\mathcal{E}^2_{\text{simult fit}}}.$$

Parameter identifiability

Structural parameter identifiability was performed using the software DAISY (Differential Algebra for Identifiability of SYstems),[39] written in REDUCE. Practical identifiability was assessed by the method of profile likelihoods,[40] that establishes whether a parameter θ is practically identifiable from a predefined set of data, and provides its confidence interval (CI) provided a certain confidence level, here set to $\alpha = 0.05$. The likelihood-based CIs are defined by:

$$\left\{\theta \middle| \mathcal{L}^2(\theta) - \mathcal{L}^2\left(\hat{\theta}\right) < \Delta_\alpha\right\} \quad \text{with} \quad \Delta_\alpha = \chi^2(\alpha, df),$$

where the threshold Δ_α is the α quantile of the χ^2-distribution with degree of freedom $(df) = 1$.

In practice, after finding the optimal parameter set $\hat{\theta}$, the profile likelihoods are computed for each parameter θ_i by fixing it to a specific value and re-optimizing all other parameters. This step is repeated for a range of values of θ_i, covering several orders of magnitude. The points at which the profile likelihood intersects the threshold Δ_α are the lower and upper bounds of the CI of θ_i. However, if the profile likelihood does not pass through the threshold, then the CI is infinite and the parameter is said to be nonidentifiable.[41]

RESULTS

A mechanism-based model of oxaliplatin PK in the ex vivo whole blood

The PBPK model of oxaliplatin in the whole blood describes the drug fate when administered ex vivo into the blood sampled from drug-naive individuals (Supplementary File S1, Section 1.1). Oxaliplatin diffuses in the tube as free Pt, then either binds to plasma proteins, or permeates into the RBCs and potentially binds to intracellular proteins.[28,29] To mimic these dynamics, our oxaliplatin PK model describes Pt levels, in the plasma and the RBC compartments, either in free or bound states (Figure 1a). Pt binding/unbinding and cellular transport rates are derived from the law of mass action and Fick's first law, respectively. Plasma or RBC intracellular proteins are assumed to be in large excess as compared with Pt quantities so that they were modeled as constant values in the equations. The binding processes were dynamically modeled as both ex vivo and clinical data showed that the steady-state hypothesis assuming proportionality between total and unbound Pt was not fulfilled (e.g. see Figure 2). The bound Pt fractions were assumed not to be able to move between compartments. Binding and unbinding rates were supposedly different between plasma (k_b^p and k_u^p) and RBC (k_b and k_u) to account for different protein content. Pt unbinding, although much slower than the other reactions, was included into the model to ensure the existence of model steady-states with non-zero values of unbound Pt, as observed in the datasets. This may represent whenever a Pt-bound protein decays, hence releasing Pt in its unbound state.

The system initial conditions were set to account for oxaliplatin being unbound in the plasma at time $t = 0$. All model parameters were tested for global identifiability using DAISY (see Methods), and resulted to be structurally identifiable without the need for initial conditions to be present.

The flowchart displayed in Figure 1c illustrates the methodological strategy undertaken for the design of our ex vivo interspecies scaling approach. It is broken down into four sequential steps with specific modeling assumptions on parameter scaling and data integration to build reliable human PBPK models from multispecies data.

Ex vivo oxaliplatin PK model faithfully fits the mouse, rat, and human datasets independently

As a first step, the ex vivo model was calibrated for each species independently, in order to retrieve the error associated with the best possible fit of each dataset, referred to as $\mathscr{E}^2$ (see Methods; strategy (1) in Figure 1c). This value served as a reference for the next parts where multispecies datasets were combined together. The model was able to closely fit each dataset, for plasma or RBC, total and ultrafiltrate Pt forms (cf. independent fits with full datasets in Table 1). The practical identifiability of each species PK parameters was also investigated (see Methods). Although all parameters were shown to be practically identifiable, many of them showed very large CIs of several orders of magnitude, which demonstrate the lack of precision for relying on a dataset from only one species (Figure 2d–f). The rat dataset was the most complete as it provided time-resolved profiles for all model variables, so that the parameter CIs were remarkably smaller than for the mouse and human datasets. In particular, the RBC binding rate k_b and the RBC uptake k_{out} resulted identifiable for human data but with large CIs.

Furthermore, we investigated the human parameter identifiability in a more realistic scenario where clinical data availability could be challenging. Thereby, this time we only used total plasma Pt levels for model calibration, according to most common measurements in the literature.[42–44] We therefore studied the effect of restraining the full human dataset (longitudinal concentrations of total and free Pt in the plasma, and total Pt in the RBCs, denoted by P_{tot}, P_f, and R_{tot}, respectively) to either P_{tot} and P_f or P_{tot} and R_{tot}, or only P_{tot}. This allowed to assess which experimental variables had the most important repercussions in terms of parameter identifiability (Figure 2g–i). Our results showed that P_f measurements were critical for the practical identifiability of the three parameters related to RBC binding, unbinding, and uptake rates (i.e., k_b, k_u, and k_{out}, respectively). Conversely, the exclusion of R_{tot} data did not hinder identifiability of any parameter, but each of them was determined within larger CIs (Table 1). Unsurprisingly, in the most data-restrained case, where we only included P_{tot}, all parameters (but one, k_{in}) became nonidentifiable.

The goodness-of-fit using only partial human data was affected in a similar manner, as quantified by an increased error $\mathscr{E}^2$ as compared to the one obtained when using all human datasets (cf. independent fits with partial datasets in Table 1).

Interspecies model scaling: purely PB strategy without use of human data did not yield accurate predictions

We have discussed, in the previous section, that patient data is often limited, and that this can substantially stretch

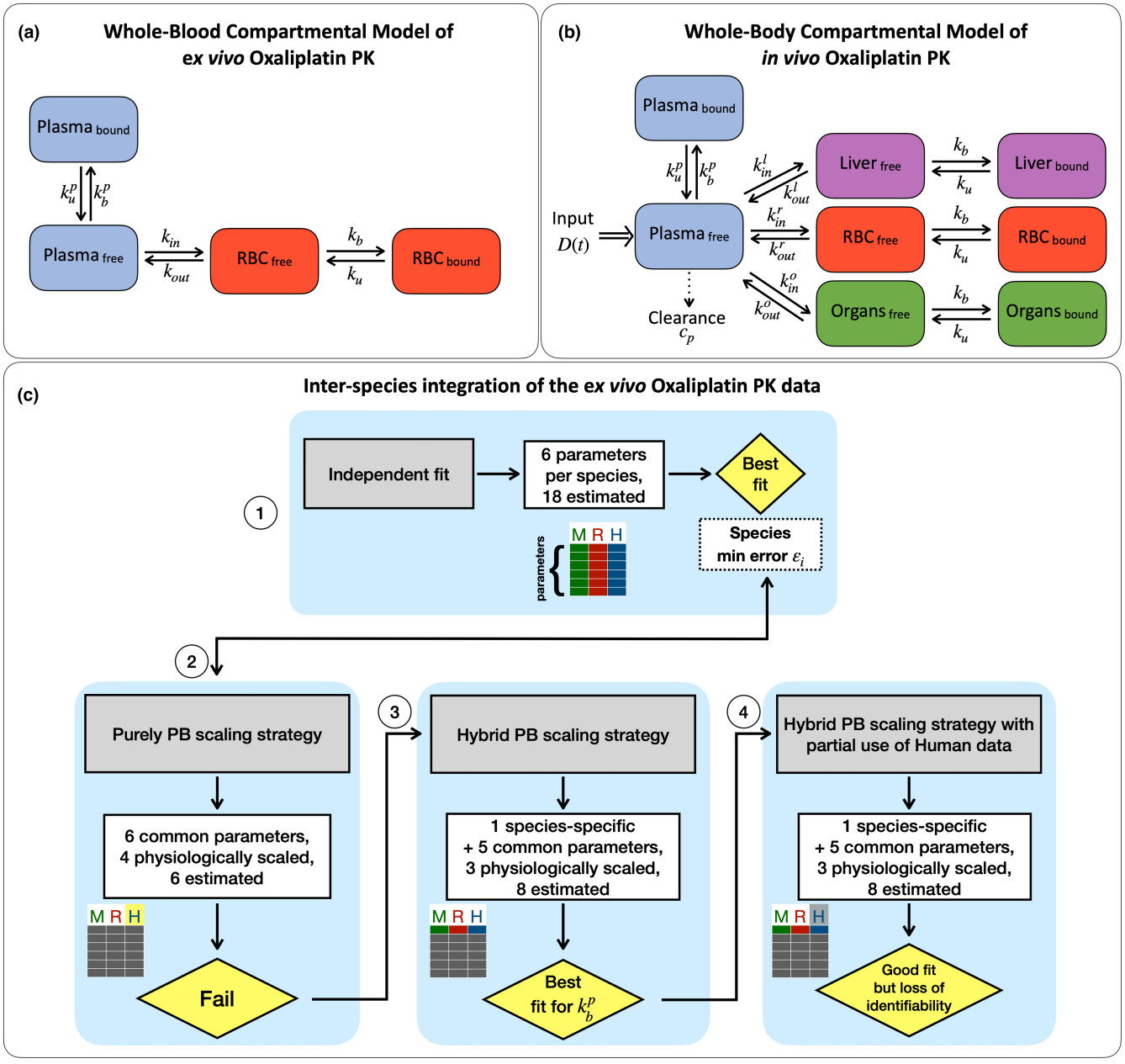

FIGURE 1 Schematic of oxaliplatin PK models and flowchart of the methodologies. (a) The ex vivo whole-blood model consists of four compartments and describes the Pt binding states in the plasma and the RBCs. Model parameters are the Pt binding and unbinding rates in the plasma (k_b^p and k_u^p), or in the RBCs (k_b and k_u), the uptake and efflux rates between the plasma and RBCs (k_{in} and k_{out}). (b) The in vivo whole-body model complements the former whole-blood model with the liver and the other non-eliminating organs. The Pt is first injected into the plasma ($D(t)$), from where a part undergoes renal clearance, and the rest transits back and forth the liver, RBC, and organs' compartments. (c) Sequence of the scaling strategies. Strategy (1) is scaling-free and consists in the independent fit of each dataset, estimating species-specific values for each model parameter (colored matrix columns), and providing the minimal model-to-data error as a reference for goodness-of-fit quantification for the following approaches. Strategy (2) is a "purely PB" scaling (i.e., based on the common estimation of the six model parameters [gray matrix columns]), using only the preclinical (mouse and rat) datasets for model fit, and retrieving the human parameters through scaling laws. This approach failed to provide a good fit. Strategies (3) and (4) are hybrid as they include a species-specific estimation of a single parameter, whereas five common parameters were calculated and subsequently scaled for each species by PB laws. They integrate the three datasets. Strategy (3) concluded that the species-specific estimation of plasma binding rate k_b^p was the only method leading to proper data fit. Strategy (4) built up on this information and undertook this methodology with partial use of human data which led to equivalent fit but partial loss of parameter identifiability. M, R, H, mouse, rat, human; PB, physiologically-based; PK, pharmacokinetic; RBC, red blood cell.

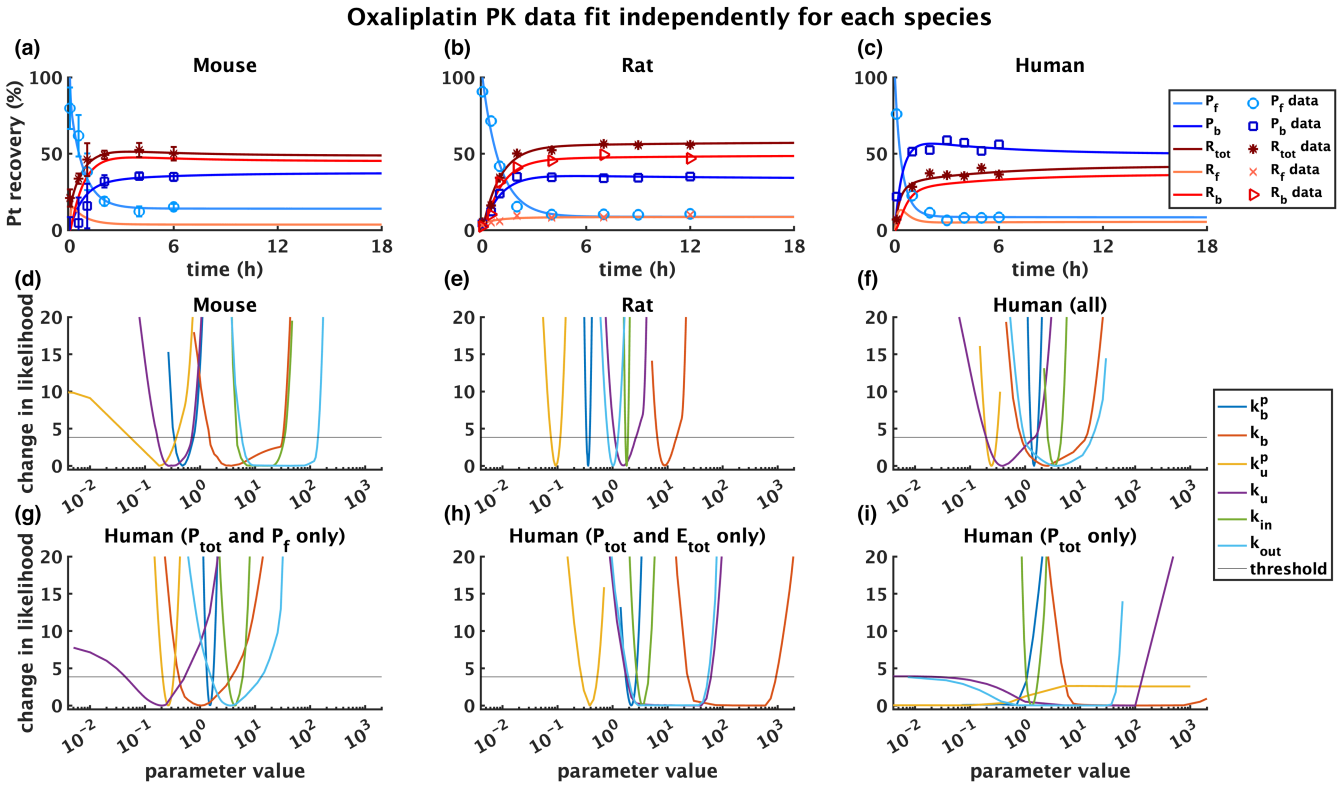

FIGURE 2 Model best fit and parameter identifiability for the ex vivo oxaliplatin PK model. Best fit for independently fitted (a) mouse, (b) rat, or (c) human datasets. Error bars represent SDs. Profile likelihood for the parameters of the single-species model based on (d) mouse, (e) rat, or (f) human whole dataset. (g–i) Profile likelihood for the parameters with partial use of the human datasets. The 95% confidence interval level for parameter identifiability is indicated by a horizontal threshold in panels d–i. PK, pharmacokinetic.

the distance between actual and predicted PK parameters, directly entailing poor in silico predictions. In response to such limitations, IVIVE concepts have emerged in view of minimizing the amount of clinical data needed to faithfully calibrate human PK models through the use of preclinical datasets, through interspecies model scaling.

We therefore developed a method based on physiological scaling laws, which conserved the structure of the ex vivo mouse, rat, and human models, adjusting the PK parameters by species-dependent physiological constants (strategy (2) in Figure 1c). More precisely, for each species S, the plasma Pt binding rate (k_b^{pS}) was assumed proportional to the total plasma protein concentration, thus saying that the reaction follows the law of mass action with circulating protein being in large excess as compared to Pt. Similarly, RBC Pt binding (k_b^S) was defined as proportional to the levels of hemoglobin, assuming that hemoglobin interspecies variation is representative of changes in total RBC protein concentrations, because it is the most abundant protein in the RBCs.[45] Pt transport rates in and out of the RBCs were re-scaled by the species-specific total RBC surface, calculated as the product of the RBC count and the surface area (SA) of a single RBC. Finally, the unbinding processes were considered as passive, hence, parameters k_u^p and k_u were assumed to be species-independent. All these considerations are then formalized by the following relations:

$$k_b^{pS} = K_b^p \times \text{Total plasma protein}^S \quad (1)$$

$$k_b^S = K_b \times \text{RBC hemoglobin}^S \quad (2)$$

$$k_{in}^S = K_{in} \times \text{RBC count}^S \times \text{SA}^S \quad (3)$$

$$k_{out}^S = K_{out} \times \text{RBC count}^S \times \text{SA}^S \quad (4)$$

where the physiological quantities were derived from the literature for all three species (Table S2 in Supplementary File S1, Section 2).

At first, we adopted a "purely PB" approach, in which the parameters of the human model were estimated from the combination of preclinical datasets. We thus estimated the six common biochemical parameters (K_b^p, K_b, K_u^p, K_u, K_{in}, and K_{out}) based on the mouse and rat observations, and then obtained human-specific PK parameters (k_b^{pH}, k_b^H, k_{in}^H, and k_{out}^H) applying the above-described PB laws (1)–(4). However, the human

TABLE 1 Best-fit par

	Units	Mouse (all)	Rat (all)	Human (all)
Independent fits (full datasets)				
Plasma binding k_b^p	$h^{(-1)}$	0.48 [0.34, 0.77]	0.36 [0.34, 0.38]	1.45 [1.28, 1.67]
RBC binding k_b	$h^{(-1)}$	3.70 [1.50, 31.81]	9.37 [6.55, 14.42]	2.61 [0.84, 12.79]
Plasma unbinding k_u^p	$h^{(-1)}$	0.18 [0.05, 0.38]	0.09 [0.08, 0.11]	0.24 [0.19, 0.31]
RBC unbinding k_u	$h^{(-1)}$	0.29 [0.16, 0.70]	1.66 [1.09, 2.69]	0.39 [0.19, 1.50]
RBC uptake k_{in}	ml/h	11.56 [4.69, 34.63]	1.80 [1.72, 1.90]	3.40 [2.58, 4.54]
RBC efflux k_{out}	ml/h	29.67 [5.77, 139.34]	1.01 [0.81, 1.26]	3.80 [0.96, 16.40]
Error ε^2	a.u.	2.62	5.28	4.38
	Units	**Human (P_{tot} and P_f)**	**Human (P_{tot} and R_{tot})**	**Human (P_{tot})**
Independent fits (partial datasets)				
Plasma binding k_b^p	$h^{(-1)}$	1.49 [1.33, 1.74]	2.19 [1.73, 2.70]	0.10 [0, 1.07]
RBC binding k_b	$h^{(-1)}$	1.50 [0.41, 3.75]	147.00 [26.28, 938.74]	9.36 [5.08, >103]
Plasma unbinding k_u^p	$h^{(-1)}$	0.26 [0.21, 0.33]	0.39 [0.27, 0.53]	0.10 [0, >103]
RBC unbinding k_u	$h^{(-1)}$	0.24 [0.04, 0.53]	10.00 [1.78, 61.23]	10.00 [0.02, 134.59]
RBC uptake k_{in}	ml/h	4.42 [3.22, 5.97]	3.55 [2.78, 4.48]	0.19 [1.04, 1.72]
RBC efflux k_{out}	ml/h	4.63 [1.58, 12.93]	9.86 [1.93, 54.49]	0.43 [0.01, 46.89]
Error ε^2	a.u.	5.25	6.37	16.43
	Units	**Mouse (all)**	**Rat (all)**	**Human (all)**
Joint inter-species fits (full datasets)				
Plasma binding k_b^p	$h^{(-1)}$	0.49 [0.06, 1.36]	0.39 [0.21, 0.62]	1.18 [0.92, 2.85]
RBC binding k_b	$h^{(-1)}$	7.70 [2.54, 57.70]	7.76 [2.56, 58.15]	8.95 [2.95, 67.09]
Plasma unbinding k_u^p	$h^{(-1)}$	0.14 [0.00, 0.37]	0.14 [0.00, 0.37]	0.14 [0.00, 0.37]
RBC unbinding k_u	$h^{(-1)}$	1.31 [0.17, 5.48]	1.31 [0.17, 5.48]	1.31 [0.17, 5.48]
RBC uptake k_{in}	ml/h	2.29 [1.46, 3.54]	1.94 [1.24, 3.00]	2.12 [1.35, 3.28]
RBC efflux k_{out}	ml/h	1.73 [0.12, 10.07]	1.47 [0.10, 8.55]	1.61 [0.11, 9.35]
Error ε^2 (individual)	a.u.	4.46	6.24	6.37
Error ε^2 (combined)	a.u.	5.55	5.55	5.55
	Units	**Mouse (all)**	**Rat (all)**	**Human (all)**
Joint interspecies fits (partial datasets)				
Plasma binding k_b^p	$h^{(-1)}$	0.47 [0.09, 1.25]	0.36 [0.21, 0.61]	1.18 [0.62, 2.32]
RBC binding k_b	$h^{(-1)}$	8.82 [3.01, 51.50]	8.89 [3.03, 51.90]	10.26 [3.50, 59.88]
Plasma unbinding k_u^p	$h^{(-1)}$	0.11 [0.00, 0.33]	0.11 [0.00, 0.33]	0.11 [0.00, 0.33]
RBC unbinding k_u	$h^{(-1)}$	1.55 [0.24, 6.07]	1.55 [0.24, 6.07]	1.55 [0.24, 6.07]
RBC uptake k_{in}	ml/h	2.16 [1.51, 3.36]	1.84 [1.28, 2.86]	2.01 [1.40, 3.12]
RBC efflux k_{out}	ml/h	1.40 [0.10, 7.21]	1.19 [0.08, 6.12]	1.30 [0.09, 6.69]
Error ε^2 (individual)	a.u.	5.01	5.37	8.17
Error $\boldsymbol{\varepsilon^2}$ (combined)	a.u.	6.34	6.34	6.34

Abbreviation: RBC, red blood cell.

predictions recovered from mouse and rat data combined in such a way, revealed a large model-to-data error (Figure 3). For mouse, rat, and human fits, respectively, the error $\mathscr{E}^2$ resulted equal to 6.22, 5.49, and 120.87; the latter being an increase of ~28 folds as compared to the best possible human fit. This demonstrated that the "purely PB" approach was inadequate to reproduce the human observations, and required the refinement of the former PB scaling assumptions.

Interspecies model scaling: combining physiologically-based scaling and partial use of human data revealed an accurate strategy

The outcome of the "purely PB" scaling hypothesis could not provide confident predictions for the considered human sets of data. We therefore investigated a novel scaling methodology that allowed us to accurately calibrate the human model integrating the human data to the preclinical (rodent) data (strategy (3) in Figure 1c).

Because PB scaling imposes a proportionality rule for any given parameter that depends on the species, here, the main idea was to relax this constraint for exactly one parameter and allow independent species-specific estimation of that one parameter, in order to maximally improve human data fit. Hence, we applied this strategy on each of the six parameters of the model. In practice, for example, if the plasma binding rate was to be fitted by species, the corresponding PB scaling law (1) would be replaced by:

$$k_b^{pS} = K_b^{pS} \times \text{Total plasma protein}^S \quad (1)$$

where K_b^{pS} now took different values for each species S. This procedure increases the number of parameters to estimate to eight, instead of six.

We assumed one PK parameter (K_b^p, K_b, K_u^p, K_u, K_{in}, K_{out}) at a time as species-specific, to explore in a mechanistic manner the validity of each PB law one-by-one. We ran the optimization algorithm for mouse, rat and human, simultaneously, and computed the goodness-of-fit $\mathcal{G}$ from the combined error $\mathcal{E}^2$ for the three species (see Methods). The overall best fit ($\mathcal{G} = 0.80$) was obtained with species-specific plasma Pt binding rates k_b^p (Table 2), which was a great improvement from the "purely PB" scaling case (strategy (2), $\mathcal{G} = 0.12$) and was closest to the reference best-fit obtained from the independent parameter estimation by species (strategy (1), $\mathcal{G} = 1$). Allowing the Pt plasma binding rate to be different for each of the three species was the only strategy that significantly increased the overall goodness-of-fit. Hence, it indicated that the corresponding PB law was largely responsible for the failure of the purely PB fit (strategy (2)).

The advantage of this approach is that the number of parameters and computational complexity stayed manageable while improving goodness-of-fit for all three species combined, with respect to any other strategy.

Notably, these findings allowed us to define an accurate interspecies scaling strategy, yet based on the whole available human dataset (Figure 4a–c). Our aim was then to investigate the impact of the partial incorporation of the human dataset on both model fit and parameter identifiability, only using P_{tot} data points (strategy (4) in Figure 1c).

On the one hand, the best-fit models were very satisfactory, providing reasonably small errors $\mathcal{E}^2$ (Figure 4d–f; joint fits in Table 1). The optimal values of each species-specific parameter were similar whether human data were included in its totality or at the bare minimum (Table 1). Even though the $\mathcal{E}^2$ error for the human model was slightly increased by 1.30-fold for partial versus full data integration, the fitness error for all species combined

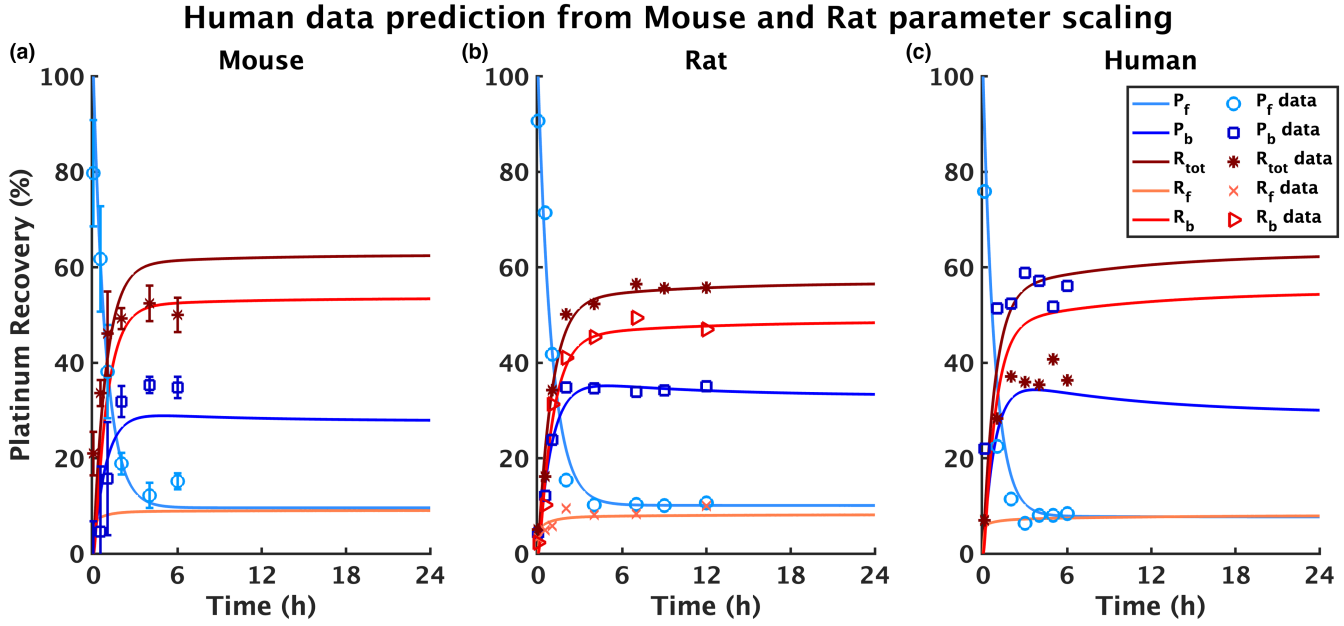

FIGURE 3 Best-fit models after calibration using the "purely PB" strategy. Human model was obtained from the rodent-derived optimal parameters corrected by human-specific scaling factors. PB, physiologically-based.

only underwent a negligible augmentation of 1.07-folds (Table 1). On the other hand, parameter identifiability was also comparatively similar: the CIs for the model informed with partial human data were slightly larger, especially for the parameter k_u^p that became nonidentifiable (Figure 4g,h).

The integration of preclinical data and the use of interspecies scaling allowed to achieve identifiability of almost all parameters of the human model solely using the P_{tot} dataset, which was instead not possible through the calibration of the human model without mouse and rat information (Figure 2i). Hence, these results suggested that such an interspecies scaling approach may prove promising in reducing the amount of patient-derived data needed to design predictive PK models.

Next, we expanded the ex vivo study to explore oxaliplatin PKs at the whole-body level. We thus built on the ex vivo whole-blood PK model and estimated human parameters translating them into an in vivo framework, according to the IVIVE principles. As a result, we developed an extended oxaliplatin whole-body PK model relevant for clinical studies.

TABLE 2 Model goodness

	Goodness-of-fit (a.u.)			
	Mouse	**Rat**	**Human**	**MRH**
Independent fit	1	1	1	1
Simultaneous fit				
Similar k's for all	0.43	0.96	0.04	0.12
Species-specific k_b^p	0.6	0.9	0.73	0.8
Species-specific k_b	0.65	0.42	0.19	0.33
Species-specific k_u^p	0.64	0.42	0.26	0.37
Species-specific k_u	0.7	0.42	0.19	0.33
Species-specific k_{in}	0.68	0.25	0.23	0.27
Species-specific k_{out}	0.63	0.44	0.21	0.35

Abbreviation: MRH, mouse, rat, human.

A mechanism-based model of oxaliplatin whole-body PKs

The model of oxaliplatin whole-body PKs in human data included the whole-blood core compartments (plasma and RBCs) which were supplemented with representation of the liver, that is an important site for both drug metabolism and metastasis for colorectal cancers, and the rest of the non-eliminating tissues, referred to as "organs" hereafter (Figure 1b). Unbound Pt in the

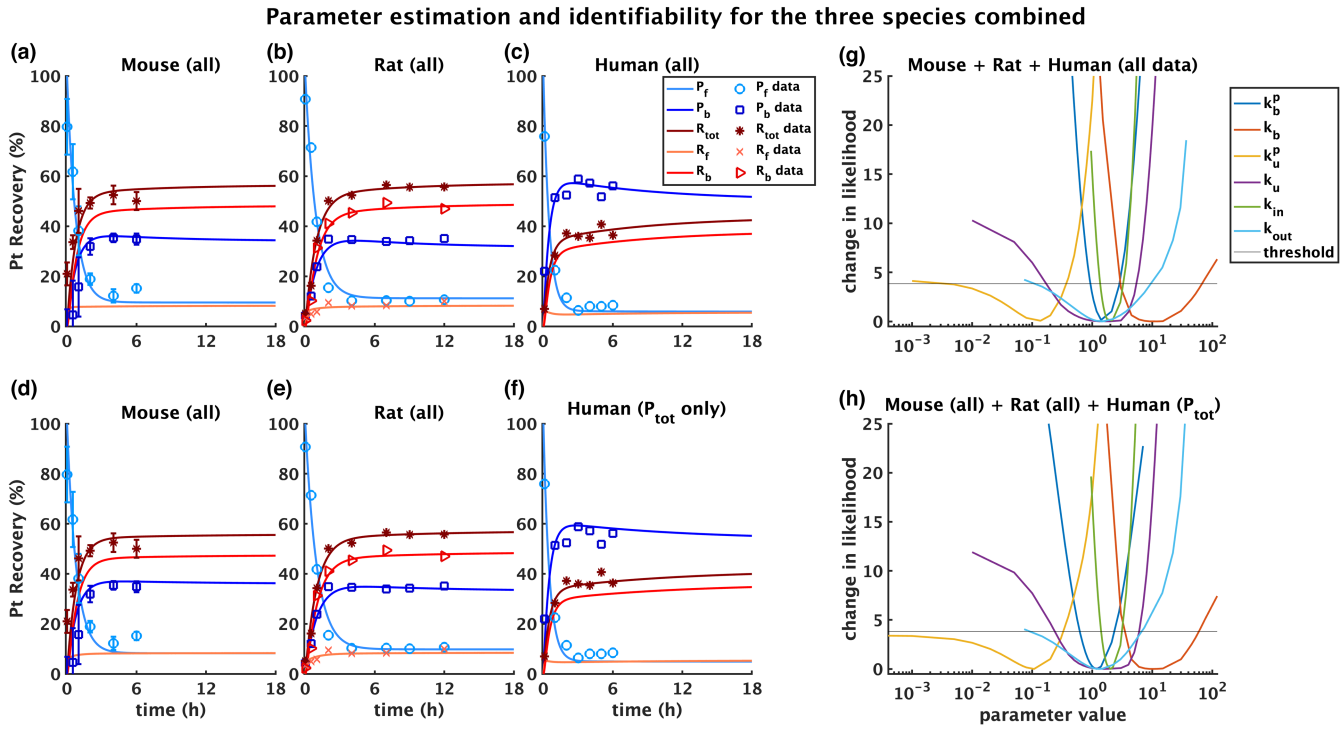

FIGURE 4 Interspecies scaling and identifiability based on mouse, rat, and human datasets combined. (a–c) Model best-fit for the hybrid PB scaling strategy where the plasma binding rates k_b^p were fitted for each species individually, using all mouse, rat, and human datasets; (e–g) model best-fit using the same approach as for (a–c) restraining the use of human data to only P_{tot}. Profile likelihoods for identifiability of the six parameters of the human model with (g) full or (h) partial data integration (see Table 1 for the optimal values and the CIs). CI, confidence intervals; PB, physiologically-based; Pt, platinum.

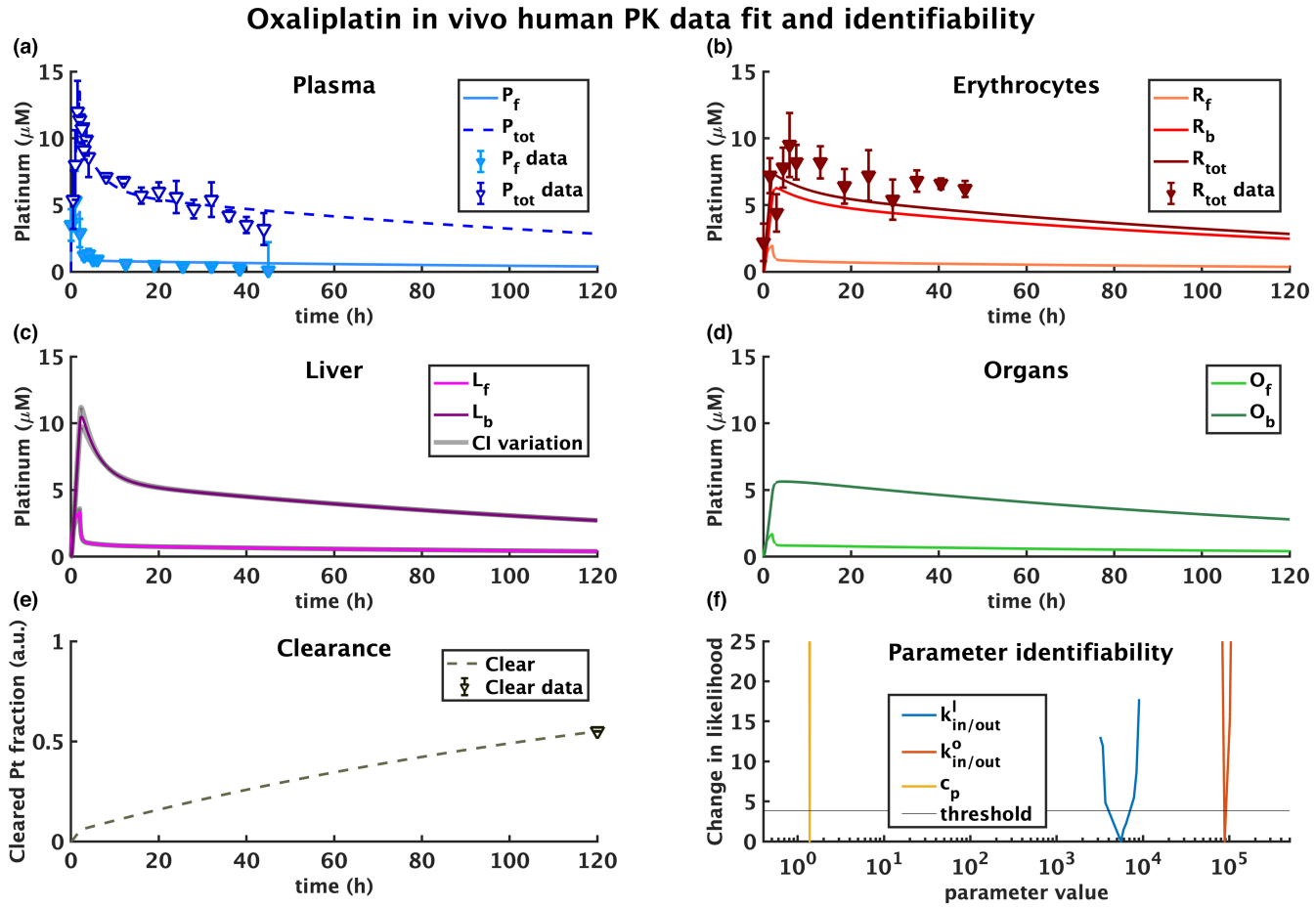

FIGURE 5 Model best-fit and parameter identifiability of the in vivo human model. (a–b) Plasma and RBC Pt levels. Open triangles correspond to data points used for parameter estimation, whereas filled symbols are the validation dataset. (c) Liver Pt levels. Gray lines represent model variation for $k^{l}_{in/out}$ values varied in its CI, with $k^{o}_{in/out}$ and c_p set to their best-fit estimation. (e) Amount of Pt cleared from the plasma compartment over time. The data point corresponds to 55% of drug cleared at the end of the simulation, as estimated from the literature. The open symbol indicates the data point was used for parameter estimation. (f) Profile likelihoods showing the identifiability of the three parameters of the in vivo model. PK, pharmacokinetic; Pt, platinum; RBC, red blood cell.

plasma could either enter or exit the liver and the organs compartments at the rates k^{l}_{in} or k^{l}_{out}, and k^{o}_{in} or k^{o}_{out}, respectively. As oxaliplatin is mainly eliminated through the kidneys, a clearance term was added in the plasma compartment (c_p).[46]

Using the study of oxaliplatin ex vivo PK in the human whole blood, we adjusted the ex vivo parameters for the whole-body scale as follows. First, the plasma and RBC Pt unbinding and binding rates (k^{p}_{u} and k^{p}_{b}, and k_u and k_b, respectively), remained unchanged from the ex vivo case because these processes followed the law of mass action. Pt transport between plasma and RBC followed Fick's first law, which states that the transport rate is proportional to the surface of contact between both compartments. Hence, the in vivo RBC transport rates, hereafter denoted as k^{r}_{in} and k^{r}_{out}, were obtained by proportionally scaling the ex vivo transport rates, k_{in} and k_{out}, using the total numbers of RBCs in the ex vivo and in vivo settings.

Concerning the liver and the organs compartments, we assumed Pt unbinding and binding rates to be the same as in the RBCs, and, for the sake of simplicity, we set the plasma uptake rate equal to the efflux rate (i.e. $k^{l}_{in} = k^{l}_{out}$ for the liver and $k^{o}_{in} = k^{o}_{out}$) for the organs (Supplementary File S1, Section 1.2).

To calibrate the oxaliplatin in vivo model, we made use of patient-derived data from ref. 36, that consisted of measurements of free and total plasma Pt (P_f and P_{tot}), and total RBC Pt (R_{tot}). Restricting our calibration to a minimal subset of data (i.e., P_{tot} only), we estimated the parameters for liver and organs transport ($k^{l}_{in/out}$ and $k^{o}_{in/out}$), and plasma clearance (c_p; Figure 5a). Both remaining datasets were then used for validation purposes (Figure 5a,b).

Time-dependent oxaliplatin intravenous injection ($D(t)$) was added to the plasma compartment. According to the original clinical trial,[36] a 2 h drug infusion was

administered to patients every 3 weeks. A single cycle was then modeled by the term:

$$D(t) = \begin{pmatrix} \text{tot\_dose}/2 & \text{for } t \le 2 \\ 0 & \text{otherwise} \end{pmatrix} \quad \text{with} \quad \text{tot\_dose} = \frac{\text{oxa\_dose} \times \text{SA}}{\text{oxa\_mol\_mass}} = 572.6 \ \mu\text{M}$$

where the oxaliplatin dose is 130 mg/m^2,[36] the oxaliplatin molar mass is 397.2858 g/mol, and the human body surface area mean across sexes (SA) is 1.75 m^2.[47]

Importantly, the total amount of oxaliplatin cleared in human 5 days post-injection was estimated to ~55% of the total dose.[46] This information was taken into account in the parameter estimation as follows. The renal clearance constraint was included in the cost function, which translated in the minimization of the following term:

$$\frac{\text{Cl}(t_f)/\text{tot\_dose} - 0.55}{\text{std\_clear}} \quad \text{with} \quad t_f = 120 \ \text{h}$$

where $\text{Cl}(t_f)$ is the quantity of Pt cleared through the kidneys at final time, and std_clear is the standard deviation of $\text{Cl}(t_f)$. The std_clear term was not documented in the literature, and was set to the minimal value ensuring the constraint was fulfilled (i.e., ±0.1% of the total dose).

We found that our model was able to fit nicely the P_{tot} data that was used for calibration. All three parameters of the models were found to be identifiable and displayed small CIs (Figure 5f). Optimal values were given by $k^{l}_{in/out} = 5589\,\text{ml/h}$ (profile likelihood-derived CI [4184, 7106]), $k^{o}_{in/out} = 88393\,\text{ml/h}$ (CI [87600, 91552]), $c_p = 1.376\,\text{h}^{-1}$ (CI [1.375, 1.377]).

We then evaluated the ability of the model to reproduce unseen data. The actual observations of free Pt in the plasma (P_f) were very close to the predicted ones (Figure 5a). On the opposite, Pt levels in RBCs (R_{tot}) were underestimated starting from 6 h after drug administration with an average deviation of ~35% (Figure 5b).

Finally, we investigated the robustness of the model predictions for Pt levels in the liver by varying the parameter $k^{l}_{in/out}$, which showed the largest CI. The parameter's variation within the lower and upper bounds values of its CI (keeping $k^{o}_{in/out}$ and c_p set to their best-fit estimation), only minimally affected the Pt time-concentration in the liver (Figure 5c).

DISCUSSION

The goal of this work was to provide a general interspecies and interscale translational methodology for reliable predictions of whole-body drug PKs in patients from both preclinical and clinical information. Two main translational questions were addressed: (1) the scaling across species, in an ex vivo setting, and (2) the multiscale ex vivo-to-in vivo extrapolation, for a given species (i.e., human).

First, we developed a PB model of oxaliplatin ex vivo PK to predict the drug transport and binding within the whole blood of three different species: mouse, rat, and human. The model successfully fitted each of the three datasets independently, hence providing a solid basis for investigating the use of preclinical data for clinical predictions. We applied a purely PB interspecies scaling method, based on species-specific blood physiological constants, in order to predict Pt whole-blood kinetics in human, solely based on mouse and rat datasets. This approach failed, so we designed a new hybrid strategy combining the estimation of one species-specific parameter with PB scaling. This time, we showed that the estimation of one parameter, for example, the Pt binding rate to plasma proteins (k^{p}_{b}) in a species-specific manner, with the other five parameters adjusted by PB scaling, was sufficient to account for the variance between the drug PKs in the three different species. Notably, our proposed methodology permitted to maximize the number of parameters common to all species, hence reducing the degrees of freedom of the approach and increasing its reliability and translational power. However, this result about species-specific k^{p}_{b} suggested that the equation used to scale Pt binding rate in the plasma was not a valid assumption. Indeed, the interspecies ratios of circulating protein concentrations were lower as compared to those of k^{p}_{b}'s (Table 1 and Table S2 in Supplementary File S1). Hence, the use of total plasma protein concentrations might not be a good proxy of Pt binding to circulating protein. More specifically, the plasma protein composition and relative proportions may vary across species which could explain the lack of predictability power of this lumped physiological value.[33,48] Moreover, circadian rhythms of circulating protein concentrations have been documented in humans,[49] rats,[50] and mice[51] and a correction for possible measurement bias might be needed. Considering that human and rat are, respectively, diurnal and nocturnal species, we could assume a phase opposition in plasma protein circadian rhythms between both. Because the maximum circulating protein concentrations in human was estimated to ~±7.5 g/dl,[49] and the minimum in Rat to 4.83 g/dl[50] which led to a ratio of 0.64. However, the ratio $k^{pRat}_{b} / k^{pHuman}_{b}$ was equal to 0.33 so that the protein variability attributable to the circadian rhythms is insufficient to account for the calculated difference in Pt plasma binding rate between rat and human (cf. strategy (3) in Table 1).

Additionally, we investigated parameter identifiability depending on the use of different datasets. We showed

that focusing on subsets of the human dataset led to degradation, if not loss, of the identifiability of several parameters. Remarkably, the key to recover identifiability for the human model was to complement those human subsets with mouse and rat information. This is highly relevant in clinical context, as the difficulties related to patient data collection must be taken into account.

Our second research question dealt with the IVIVE challenge and aimed to predict oxaliplatin whole-body PKs in human. For that, the ex vivo model was incorporated into a larger whole-body in vivo PBPK model accounting for the liver and other non-eliminating organs. The PK parameters of plasma and RBC binding/unbinding were used directly into the new model, whereas RBC transport parameters were scaled from the ex vivo model according to RBC surfaces. The three remaining model parameters were calibrated to in vivo human data on total plasma Pt time-course profiles which were well fitted. Furthermore, the best-fit model was able to achieve a good fit to unseen observations on free plasma Pt kinetics. Regarding RBCs, the model underestimated Pt data, which indicated that the scaling method of the RBC transport parameters may need to be refined. The liver predictions also have an added value because, according to our knowledge, those data have not yet been assessed in patients with cancer due to technical hurdles. Such information may be critical in the context of malignancies associated with liver metastases. Trustworthy simulation of liver drug concentrations is essential for estimating patient-specific dosimetry and timing. Thus, experimental confirmation of our results would be of high importance.

The physiological relevance of our parameter estimates is detailed hereafter by comparison to previously reported values. Our whole-body PK model led to oxaliplatin ultrafiltrate clearance of 4.0702 L/h. This was comparable to the values computed in studies using bi-compartment models (i.e., 4.81 ± 1.93,[52] and 8.5 ± 0.29 L/h in women and 14.1 ± 1.15 L/h in men).[53] It was slightly lower than the literature values, reported in classical PK analyses based on model-independent approaches, which ranged from 9.3 to 26.5 L/h.[31,46] Those studies do not explicitly consider the dynamics of Pt binding so that comparison of binding parameters were not possible. Furthermore, published compartmental models include different numbers of compartments with different volumes as compared to our model so that transport parameters were not comparable.

One promising expansion of the current work would envisage the applicability of this methodology to other drugs, because the framework we presented here is rather general. Accurately integrating preclinical results into the design of mechanistic whole-body human drug PK models would allow for the optimization of clinical trial design, in a cost- and time-effective manner. Importantly, such a tool allows to integrate patient biomarkers, covariates, pharmacogenomics, or molecular information, such as liver enzyme activity, for individualized prediction of drug PKs. The model ability to describe and mechanistically explain interpatient variability is crucial to predict drug response and resistance toward treatment personalization. Another important aspect that revealed decisive in therapy response is related to the circadian timing system, that rhythmically controls most physiological processes over the 24 h span.[25] The circadian rhythms in tumor and healthy tissues may largely affect drug response and can be included in mechanistic PK/PD models to strategically exploit them for drug timing optimization.[54] Furthermore, oxaliplatin PKs, antitumor efficacy, and toxicities were shown to depend on the dosing-time both in preclinical and clinical studies.[30,54] Such a circadian-related variability could not be investigated in the present study as timing of blood sampling, although reported for the mouse experiments (ZT3, Methods section), was not indicated either in the rat or in the human datasets. Hence, further mechanism-based circadian studies of oxaliplatin PKs are required.

In conclusion, our work incorporated and unified concepts of both interspecies and IVIVE scaling, and illustrated a modeling framework based on QSP that overcomes the common bottlenecks encountered in either field. The proposed approaches and their application into the clinics will mark an important achievement in the rational design of more effective cancer treatment strategies.

AUTHOR CONTRIBUTIONS

S.C., R.H., and A.B. wrote the manuscript. A.B. designed the research. S.C., R.H., S.D., X.L., and E.C. performed the research. S.C., R.H., X.L., E.C., S.D., and A.B. analyzed the data. S.C. and R.H. contributed new analytical tools.

ACKNOWLEDGMENTS

The authors would like to thanks Dr Sergio Corridore (INSERM U900, Paris, France) and Dr Julien Martinelli (Aalto University, Helsinki, Finland) for helpful discussions.

FUNDING INFORMATION

This work was supported by the postdoctoral fellowship program of the French Charity "Fondation ARC pour la Recherche sur le Cancer," the French Plan Cancer through the ATIP-Avenir programme, the French National Institute for Health and Medical Research (INSERM), and by the Engineering and Physical Sciences Research Council (EPSRC) and Medical Research Council (MRC) through the Centre for Doctoral Training in Mathematics for Real-World Systems at the University of Warwick (UK).

CONFLICT OF INTEREST

The authors declared no competing interests for this work.

ORCID

Simona Catozzi https://orcid.org/0000-0001-6132-5712

REFERENCES

1. Lowe PJ. *Quantitative Pharmacology: An Introduction to Integrative Pharmacokinetic-Pharmacodynamic Analysis*. Wiley-Blackwell; 2012.
2. Jones HM, Rowland-Yeo K. Basic concepts in physiologically based pharmacokinetic modeling in drug discovery and development. *CPT Pharmacometrics Syst Pharmacol*. 2013;2(8):1-12. doi:10.1038/PSP.2013.41
3. Yoshida K, Budha N, Jin JY. Impact of physiologically based pharmacokinetic models on regulatory reviews and product labels: frequent utilization in the field of oncology. *Clin Pharmacol Ther*. 2017;101(5):597-602. doi:10.1002/cpt.622
4. Musuamba FT, Skottheim Rusten I, Lesage R, et al. Scientific and regulatory evaluation of mechanistic in silico drug and disease models in drug development: building model credibility. *CPT Pharmacometrics Syst Pharmacol*. 2021;10:804-825. doi:10.1002/PSP4.12669
5. Us Food and Drug Administration (FDA). The Use of Physiologically Based Pharmacokinetic Analyses – Biopharmaceutics Applications for Oral Drug Product Development, Manufacturing Changes, and Controls. Tech. rep. 2020. https://www.fda.gov/regulatory-information/search-fda-guidance-documents/use-physiologically-based-pharmacokinetic-analyses-biopharmaceutics-applications-oral-drug-product
6. European Medicines Agency (EMA). Guideline on the reporting of physiologically based pharmacokinetic (PBPK) modelling and simulation. Tech. rep. 2018.
7. Quignot N, Bois FY. A computational model to predict rat ovarian steroid secretion from in vitro experiments with endocrine disruptors. *PloS One*. 2013;8(1):e53891. doi:10.1371/journal.pone.0053891
8. Chang X, Tan Y-M, Allen DG, et al. IVIVE: facilitating the use of in vitro toxicity data in risk assessment and decision making. *Toxics*. 2022;10(5):232. doi:10.3390/toxics10050232
9. Lin JH, Yamazaki M. Role of P-glycoprotein in pharmacokinetics. *Clin Pharmacokinet*. 2003;42(1):59-98. doi:10.2165/00003088-200342010-00003
10. Johnson TN, Small BG, Berglund EG, Rowland Yeo K. A best practice framework for applying physiologically-based pharmacokinetic modeling to pediatric drug development. *CPT Pharmacometrics Syst Pharmacol*. 2021;10(9):967-972. doi:10.1002/psp4.12678
11. Karelina T, Demin O, Nicholas T, Lu Y, Duvvuri S, Barton HA. A translational systems pharmacology model for a β kinetics in mouse, monkey, and human. *CPT Pharmacometrics Syst Pharmacol*. 2017;6(10):666-675. doi:10.1002/psp4.12211
12. Lindauer A, Valiathan CR, Mehta K, et al. Translational pharmacokinetic/pharmacodynamic modeling of tumor growth inhibition supports dose-range selection of the anti–PD-1 antibody pembrolizumab. *CPT Pharmacometrics Syst Pharmacol*. 2017;6(1):11-20. doi:10.1002/psp4.12130
13. West GB, Woodruff WH, Brown JH. Allometric scaling of metabolic rate from molecules and mitochondria to cells and mammals. *Proc Natl Acad Sci*. 2002;99(Suppl 1):2473-2478. doi:10.1073/pnas.012579799
14. Lledo-Garcia R, Dixon K, Shock A, Oliver R. Pharmacokinetic-pharmacodynamic modelling of the anti-FcRn monoclonal antibody rozanolixizumab: translation from preclinical stages to the clinic. *CPT Pharmacometrics Syst Pharmacol*. 2021;11:116-128. doi:10.1002/psp4.12739
15. Chen T, Mager DE, Kagan L. Interspecies modeling and prediction of human exenatide pharmacokinetics. *Pharm Res*. 2013;30(3):751-760. doi:10.1007/s11095-012-0917-z
16. Malik PRV, Edginton AN. Physiologically-based vs. allometric scaling for the prediction of infliximab pharmacokinetics in pediatric patients. *CPT Pharmacometrics Syst Pharmacol*. 2019;8(11):835-844. doi:10.1002/psp4.12456
17. Hanafin PO, Jermain B, Hickey AJ, et al. A mechanism-based pharmacokinetic model of remdesivir leveraging interspecies scaling to simulate COVID-19 treatment in humans. *CPT Pharmacometrics Syst Pharmacol*. 2021;10(2):89-99. doi:10.1002/psp4.12584
18. Alskär O, Karlsson MO, Kjellsson MC. Model-based interspecies scaling of glucose homeostasis. *CPT Pharmacometrics Syst Pharmacol*. 2017;6(11):778-786. doi:10.1002/psp4.12247
19. Naritomi Y, Sanoh S, Ohta S. Utility of chimeric mice with humanized liver for predicting human pharmacokinetics in drug discovery: comparison with in vitro–in vivo extrapolation and allometric scaling. *Biol Pharmaceut Bull*. 2019;42(3):327-336. doi:10.1248/bpb.b18-00754
20. Krauss M, Hofmann U, Schafmayer C, et al. Translational learning from clinical studies predicts drug pharmacokinetics across patient populations. *NPJ Syst Biol Appl*. 2017;3(1):1-11. doi:10.1038/s41540-017-0012-5
21. Feasel MG, Lawrence RJ, Kristovich RL. Translational Human Health Assessment of Carfentanil Using an Experimentally Refined PBPK Model. Tech. rep. ARMY EDGEWOOD CHEMICAL BIOLOGICAL CENTER APG MD National Inst on Drug Abuse, 2018. https://apps.dtic.mil/sti/pdfs/AD1060142.pdf
22. Chang H-Y, Wu S, Meno-Tetang G, Shah DK. A translational platform PBPK model for antibody disposition in the brain. *J Pharmacokinet Pharmacodyn*. 2019;46(4):319-338. doi:10.1007/s10928-019-09641-8
23. Venkatakrishnan K, Friberg LE, Ouellet D, et al. Optimizing oncology therapeutics through quantitative translational and clinical pharmacology: challenges and opportunities. *Clin Pharmacol Ther*. 2015;97(1):37-54. doi:10.1002/cpt.7
24. Culy CR, Clemett D, Wiseman LR. Oxaliplatin. *Drugs*. 2000;60(4):895-924. doi:10.2165/00003495-200060040-00005
25. Ballesta A, Innominato PF, Dallmann R, Rand DA, Lévi F. Systems chronotherapeutics. *Pharmacol Rev*. 2017;69:161-199. doi:10.1124/pr.116.013441
26. Özdemir BC, Csajkag, Dotto GP, Wagner AD. Sex differences in efficacy and toxicity of systemic treatments: an undervalued issue in the era of precision oncology. *J Clin Oncol*. 2018;36:2680-2683. doi:10.1200/JCO.2018.78.3290
27. Giacchetti S, Dugué PA, Innominato PF, et al. Sex moderates circadian chemotherapy effects on survival of patients with metastatic colorectal cancer: a meta-analysis. *Ann Oncol*. 2012;23(12):3110-3116. doi:10.1093/annonc/mds148

28. Allain P, Heudi O, Cailleux A, et al. Early biotransformations of oxaliplatin after its intravenous administration to cancer patients. *Drug Metab Dispos*. 2000;28(11):1379-1384.
29. Wang J, Tao J, Jia S, Wang M, Jiang H, Du Z. The protein-binding behavior of platinum anticancer drugs in blood revealed by mass spectrometry. *Pharmaceuticals*. 2021;14(104):1-16. doi:10.3390/ph14020104
30. Lévi F, Metzger G, Massari C, Milano G. Oxaliplatin. *Clin Pharmacokinet*. 2000;38:1-21.
31. Graham MA, Lockwood GF, Greenslade D, Brienza S, Bayssas M, Gamelin E. Clinical pharmacokinetics of oxaliplatin: a critical review. *Clin Cancer Res*. 2000;6(4):1205-1218.
32. Thiel C, Schneckener S, Krauss M, et al. A systematic evaluation of the use of physiologically based pharmacokinetic modeling for cross-species extrapolation. *J Pharm Sci*. 2015;104(1):191-206. doi:10.1002/jps.24214
33. Espósito BP, Najjar R. Interactions of antitumoral platinum-group metallodrugs with albumin. *Coord Chem Rev*. 2002;232(1):137-149. doi:10.1016/S0010-8545(02)00049-8
34. Luo FR, Wyrick SD, Chaney SG. Biotransformations of oxaliplatin in rat blood in vitro. *J Biochem Mol Toxicol*. 1999;13(3–4):159-169.
35. Pendyala L, Creaven PJ. In vitro cytotoxicity, protein binding, red blood cell partitioning, and biotransformation of oxaliplatin. *Cancer Res*. 1993;53(24):5970-5976.
36. Massari C, Brienza S, Rotarski M, et al. Pharmacokinetics of oxaliplatin in patients with normal versus impaired renal function. *Cancer Chemother Pharmacol*. 2000;45(2):157-164. doi:10.1007/s002800050024
37. Gareth J, Witten D, Hastle T, Tibshirani R. *An Introduction to Statistical Learning: with Applications in R*. Springer; 2013.
38. Beyer H-G, Sendhoff B. Covariance matrix adaptation revisited–the CMSA evolution strategy. *International Conference on Parallel Problem Solving from Nature*. Springer; 2008:123-132.
39. Bellu G, Saccomani MP, Audoly S, D'Angiò L. DAISY: a new software tool to test global identifiability of biological and physiological systems. *Comput Methods Programs Biomed*. 2007;88(1):52-61. doi:10.1016/j.cmpb.2007.07.002
40. Raue A, Kreutz C, Maiwald T, et al. Structural and practical identifiability analysis of partially observed dynamical models by exploiting the profile likelihood. *Bioinformatics*. 2009;25(15):1923-1929. doi:10.1093/bioinformatics/btp358
41. Stryhn H, Christensen J. Confidence intervals by the profile likelihood method, with applications in veterinary epidemiology. *Proceedings of the 10th International Symposium on Veterinary Epidemiology and Economics, Vina del Mar*. Vol 208, International Symposia on Veterinary Epidemiology and Economics; 2003.
42. Marty M. "L-OHP phase I study". Debiopharm/Sanofi Report No. TDU3099 (1989).
43. Gamelin E, Bouil AL, Boisdron-Celle M, et al. Cumulative pharmacokinetic study of oxaliplatin, administered every three weeks, combined with 5-fluorouracil in colorectal cancer patients. *Clin Cancer Res*. 1997;3(6):891-899.
44. Misset JL, Allain P. "Pharmacokinetics, urinary, and fecal excretion of oxaliplatin in cancer patients". Debiopharm/Sanofi Report No. TDR3500 (1995).
45. Bryk AH, Wisniewski JR. Quantitative analysis of human red blood cell proteome. *J Proteome Res*. 2017;16(8):2752-2761.
46. Raymond E, Chaney SG, Taamma A, Cvitkovic E. Oxaliplatin: a review of preclinical and clinical studies. *Ann Oncol*. 1998;9:1053-1071. doi:10.1023/A:1008213732429
47. Mosteller RD. Simplified calculation of body-surface area. *N Engl J Med*. 1987;317:1098.
48. Martinez MN. Factors influencing the use and interpretation of animal models in the development of parenteral drug delivery systems. *AAPS J*. 2011;13(4):632-649. doi:10.1208/s12248-011-9303-8
49. Touitou Y, Touitou C, Bogdan A, et al. Differences between young and elderly subjects in seasonal and circadian variations of Total plasma proteins and blood volume as reflected by hemoglobin, hematocrit, and erythrocyte counts. *Clin Chem*. 1986;32(5):801-804.
50. Minematsu S, Watanabe M, Tsuchiya N, Watanabe M, Amagaya S. Diurnal variations in blood Chemical items in Sprague-Dawley rats. *Exp Anim*. 1995;44(3):223-232.
51. Swoyer J, Haus E, Sackett-Lundeen L. Circadian reference values for hematologic parameters in several strains of mice. *Prog Clin Biol Res*. 1987;227A:281-296.
52. Liu J, Kraut E, Bender J, et al. Pharmacokinetics of oxaliplatin (NSC 266046) alone and in combination with paclitaxel in cancer patients. *Cancer Chemother Pharmacol*. 2002;49(5):367-374. doi:10.1007/s00280-002-0426-6
53. Bastian G, Barrail A, Urien S. Population pharmacokinetics of oxaliplatin in patients with metastatic cancer. *Anticancer Drugs*. 2003;14:817-824. doi:10.1097/01.cad.0000099000.92896.5d
54. Lévi F, Okyar A, Dulong S, Innominato PF, Clairambault J. Circadian timing in cancer treatments. *Annu Rev Pharmacol Toxicol*. 2010;50:377-421. doi:10.1146/annurev.pharmtox.48.113006.094626

SUPPORTING INFORMATION

Additional supporting information can be found online in the Supporting Information section at the end of this article.

How to cite this article: Catozzi S, Hill R, Li X-M, Dulong S, Collard E, Ballesta A. Interspecies and in vitro-in vivo scaling for quantitative modeling of whole-body drug pharmacokinetics in patients: Application to the anticancer drug oxaliplatin. *CPT Pharmacometrics Syst Pharmacol*. 2023;12:221-235. doi:10.1002/psp4.12895